Scilight

Materials and Sustainability

https://www.sciltp.com/journals/matsus

Supplementary Materials

Deposition-Pathway-Controlled Interfacial Chemistry and Scalability of Spatial-Atomic-Layer-Deposited Cu_2O Hole Transport Layers in Inverted Perovskite Solar Cells

Neeru Chaudhary [1,2,†], Ahmed Shahin [2,3,†], Navdeep Goyal [1] and Kevin P. Musselman [2,3,*]

[1] Department of Physics, Panjab University, Chandigarh 160014, India
[2] Department of Mechanical and Mechatronics Engineering, University of Waterloo, Waterloo, ON N2L 3G1, Canada
[3] Waterloo Institute for Nanotechnology, University of Waterloo, Waterloo, ON N2L 3G1, Canada
* Correspondence: kevin.musselman@uwaterloo.ca
† These authors contributed equally to this work.

How To Cite: Chaudhary, N.; Shahin, A.; Goyal, N.; et al. Deposition-Pathway-Controlled Interfacial Chemistry and Scalability of Spatial-Atomic-Layer-Deposited Cu_2O Hole Transport Layers in Inverted Perovskite Solar Cells. *Materials and Sustainability* **2026**, *2*(4), 8. https://doi.org/10.53941/matsus.2026.100008

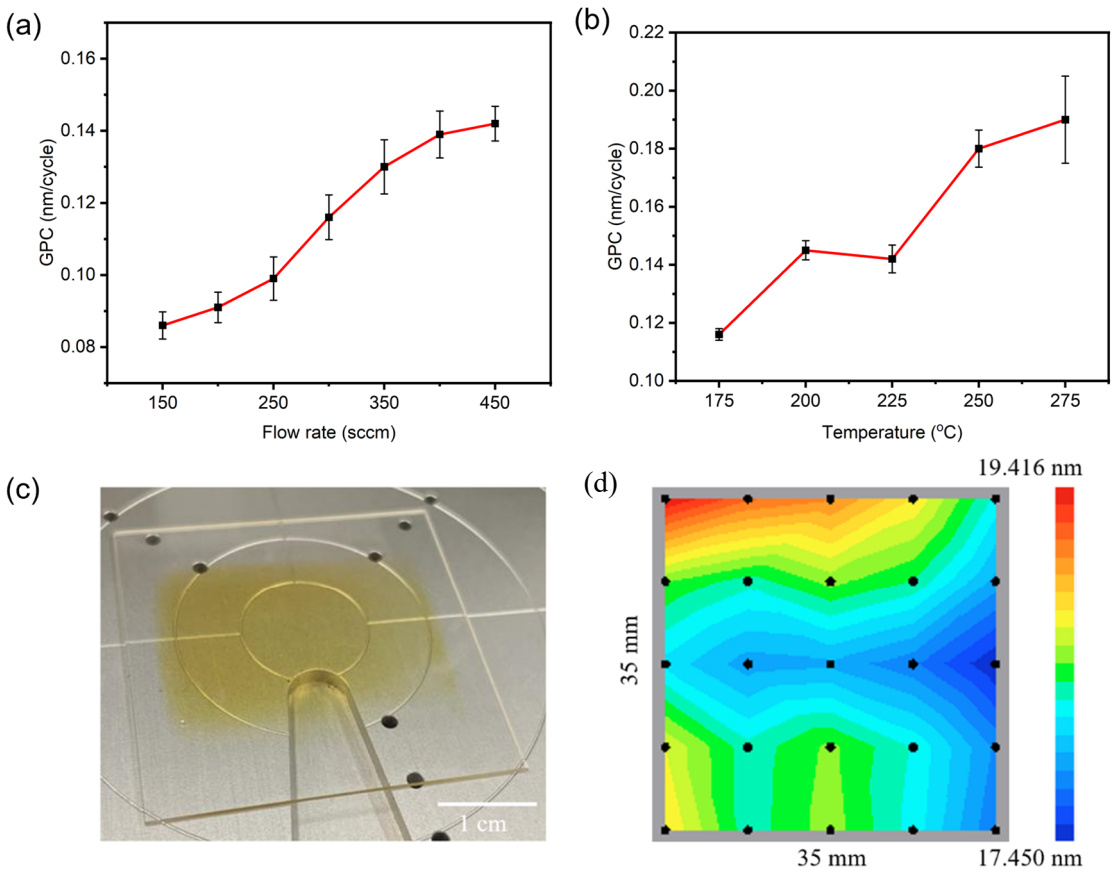

Figure S1. Growth characteristics and spatial uniformity of AP-SALD Cu_2O films. Growth per cycle (GPC) as a function of (**a**) Cu precursor flow rate and (**b**) deposition temperature. Error bars represent spatial variations in film thickness. (**c**) Photograph of a deposited Cu_2O film and (**d**) corresponding thickness map over a 35 × 35 mm^2 area.

Copyright: © 2026 by the authors. This is an open access article under the terms and conditions of the Creative Commons Attribution (CC BY) license (https://creativecommons.org/licenses/by/4.0/).
Publisher's Note: Scilight stays neutral with regard to jurisdictional claims in published maps and institutional affiliations.

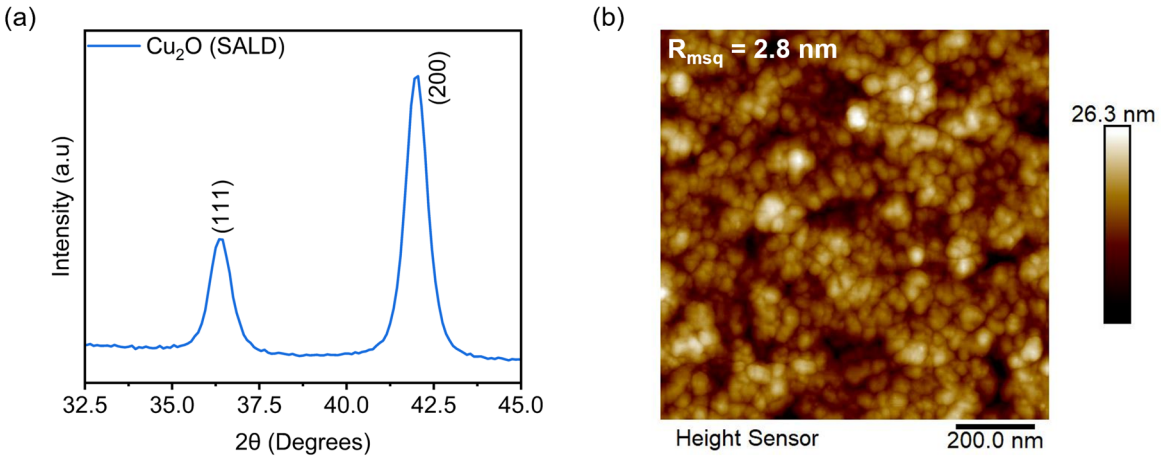

Figure S2. Confirmation of conformal Cu_2O deposition via AP-SALD. (**a**) GIXRD measurement showing (111) and (200) characteristic reflections of Cu_2O. (**b**) AFM scan of Cu_2O, deposited on ITO. The Cu_2O film on ITO had a root mean square surface roughness of 2.8 nm. The Cu_2O films for this analysis were approximately 40 nm thick.

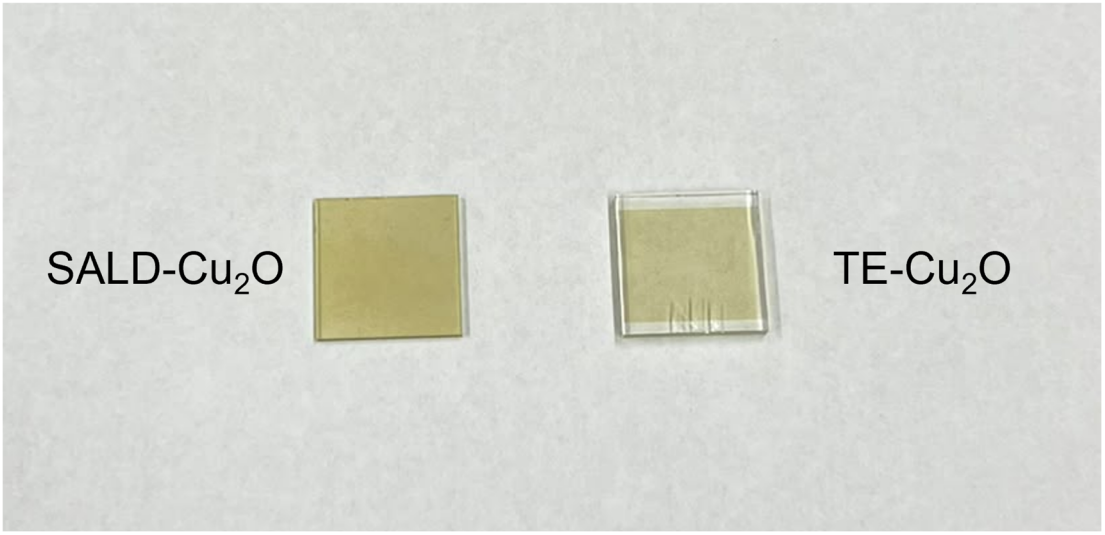

Figure S3. Photograph of Cu_2O thin films prepared by atmospheric-pressure spatial atomic layer deposition (SALD-Cu_2O, **left**) and thermal evaporation followed by oxidation (TE-Cu_2O, **right**).

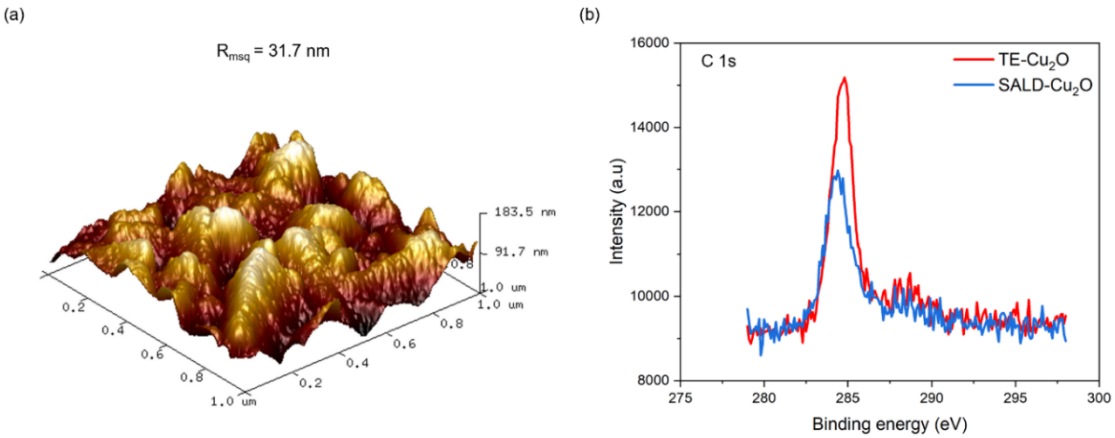

Figure S4. (**a**) 3D AFM image of TE-Cu_2O showing an RMS roughness of 31.7 nm on FTO/glass. (**b**) XPS C 1s spectra of TE-Cu_2O and SALD-Cu_2O, showing a higher carbon signal for TE-Cu_2O (10 s of Ar sputtering).

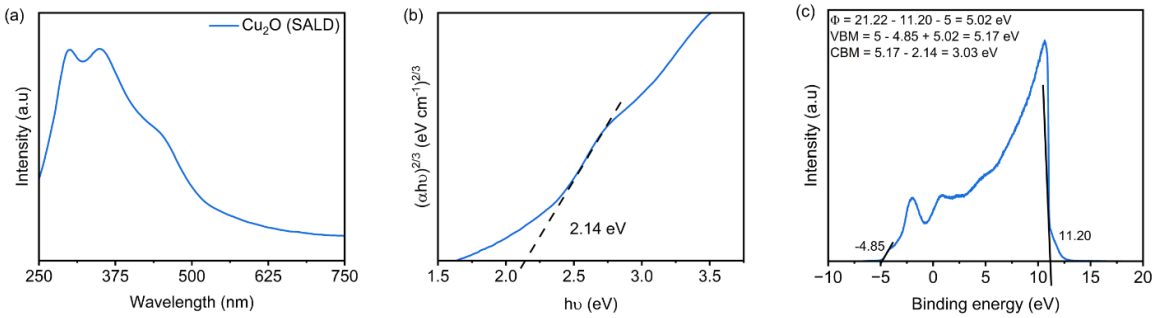

Figure S5. Optical and electronic structure of SALD-Cu_2O thin films. (**a**) UV–vis absorption spectrum of SALD-Cu_2O. (**b**) Direct-forbidden transition Tauc analysis $(\alpha h\nu)^{2/3}$ vs $h\nu$, yielding an optical bandgap of 2.14 eV from the linear extrapolation to $(\alpha h\nu)^{2/3} = 0$. (**c**) Ultraviolet photoelectron spectroscopy (UPS, He I, $h\nu = 21.22$ eV) showing the secondary electron cutoff and valence-band edge offset from the Fermi level used to determine the work function and valence band maximum relative to vacuum; the conduction band minimum is then obtained using the measured bandgap.

Table S1. Comparison of average pinhole size and density in $FAMAPbI_3$ and $MAPbI_3$ films deposited on thermally evaporated and oxidized Cu_2O (TE-Cu_2O) and spatial-ALD-deposited Cu_2O (SALD-Cu_2O), determined from SEM image analysis.

Perovskite	Cu_2O	Pinhole Size (nm)	Density (um^2)
$FAMAPbI_3$	TE	93.8	12.8
$FAMAPbI_3$	SALD	113.9	22.3
$MAPbI_3$	TE	65.6	33.0
$MAPbI_3$	SALD	N/A	N/A